Journal Pre-proof

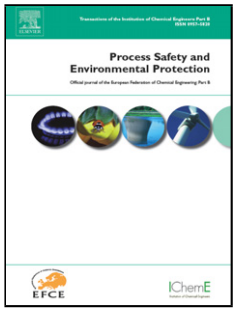

Selection of operational parameters for a smart spraying system to control airborne PM_{10} and $PM_{2.5}$ dusts in underground coal mines

Dominik Bałaga, Michał Siegmund, Marek Kalita, Ben J. Williamson, Andrzej Walentek, Marcin Małachowski

PII: S0957-5820(20)31791-2

DOI: https://doi.org/10.1016/j.psep.2020.10.001

Reference: PSEP 2506

To appear in: *Process Safety and Environmental Protection*

Received Date: 5 June 2020

Revised Date: 16 September 2020

Accepted Date: 3 October 2020

Please cite this article as: { doi: https://doi.org/

Selection of operational parameters for a smart spraying system to control airborne PM_{10} and $PM_{2.5}$ dusts in underground coal mines

Bałaga Dominik, Siegmund Michał, Kalita Marek, Williamson Ben J, Walentek Andrzej, Małachowski Marcin

Bałaga Dominik
KOMAG Institute of Mining Technology, Pszczynska 37, 44-101 Gliwice, Poland, dbalaga@komag.eu
Siegmund Michał
KOMAG Institute of Mining Technology, Pszczynska 37, 44-101 Gliwice, Poland, msiegmund@komag.eu
Kalita Marek
KOMAG Institute of Mining Technology, Pszczynska 37, 44-101 Gliwice, Poland, mkalita@komag.eu
Williamson Ben J.
University of Exeter – Cornwall Campus, Cornwall TR10 9FE, United Kingdom, b.j.williamson@exeter.ac.uk
Walentek Andrzej
Central Mining Institute, Plac Gwarków, 40-166 Katowice, Poland, awalentek@gig.eu
Małachowski Marcin
Institute of Innovative Technologies EMAG, Leopolda 31, 40-189 Katowice, Poland, marcin.malachowski@ibemag.pl

Graphical abstract

Selection of operational parameters for a smart spraying system to control airborne PM_{10} and $PM_{2.5}$ dusts in underground coal mines

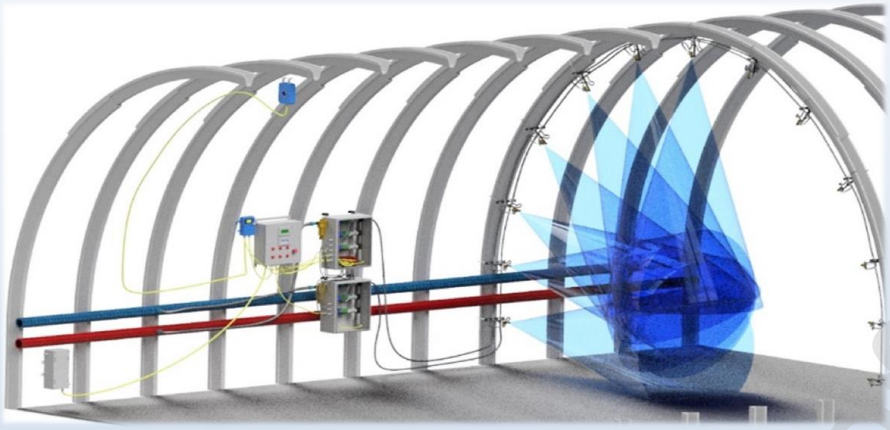

3D visualisation and functionall tests of the SSD-1

Underground in situ-tests

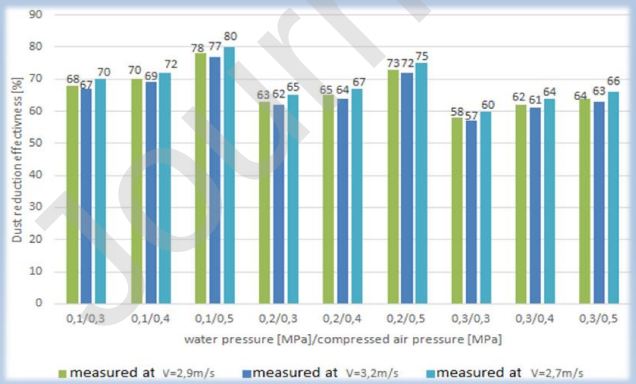

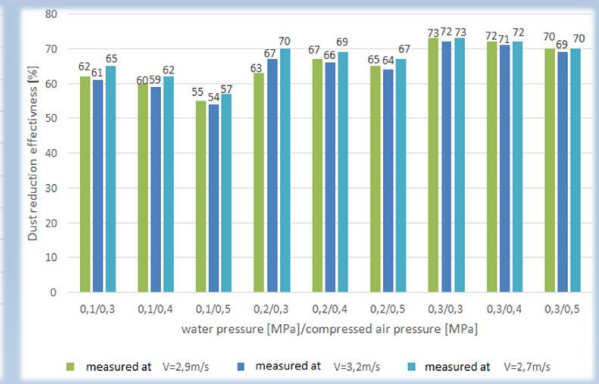

Effectiveness in reduction of PM2.5 (left) and PM10 (right) dust concentration

Highlights

- The spraying device was developed, to remove dust particles from mine air
- Stand tests on the smart spraying device prototype were positive
- Fractional drops distribution was tested on the laboratory stand test
- Drops absorption surface area were determined
- A method for selecting the drops size for dust concentration was developed

Airborne dust in underground hard coal mines is an ongoing explosion and respiratory health hazard. The latest design solution for controlling dusts, the smart spraying system, is described. From the results of stand tests, the main factors determining the efficiency of the new device are: 1) the integrated real-time acquisition of dust particle size and concentration data, determined using a new optical dust meter; 2) the fractional distribution of water droplets; and 3) the selection of droplet size to capture PM_{10} and $PM_{2.5}$. The latter two factors are automatically controlled, based on dust measurements, by varying the pressure of water and compressed air supplied to the sprayer nozzles. The effects of varying these parameters and the results of stand tests are presented. The spraying device was tested for the effectiveness of PM2.5 dust and PM10 dust reduction in underground conditions in the KWK Pniówek mine. The tests were based on the following Polish Standards: PN-91/Z-04030/05 and PN91/Z-04030/06, which define the methodology for measurements of inhalable and respirable dust at workplaces using the filtration-weighing method to determine the concentration of inhalable and respirable dust with the spraying system on and off. The results showed that the assumed objective, i.e. development of a dust control device that would reduce PM2.5 dust (by min. 25%) and PM10 dust (by min. 20%) more effectively than the currently used solutions, was achieved in the project. At the same time, the device, due to application of dust sensor, continuously adjusts the parameters of spraying streams to the dust concentration level, optimizing the consumption of water and compressed air. Similar results in reduction of PM10 and PM2.5 dust, with an average effectiveness of over 60% is the undoubted advantage of the device.

Keywords: coal dust; particle diameter; dust suppression; water-air spraying device

1. Introduction

There are a number of hazards associated with underground coal mining, coal dust is one of them. Its generation, , has generally increased over time due to mechanization of mining processes and higher productivity. The dust is lofted and moved around by air currents, increasing the risk of explosions and respiratory diseases of miners. The likelihood of explosions is greatest where there are high concentrations of combustible dust, an oxidizer (mine air) and an ignition source, in confined space being particularly hazardous [Cybulski, 1973]. Dust explosions are rare and difficult to predict but their effects can be extremely dangerous for mine personnel and equipment. Historically, the most serious disasters related to coal dust explosions were in the Henkeiko mine, Manchuria, in 1942 (1,527 deaths) and in the Courries mine in France, in 1906 (1099 deaths) [Rojek, 2012] and in recent years in Mexico, Pasta De Conchos, 2006; U.S., Upper Big Branch, 2010r, Turkey in Soma, in 2014.

Pneumoconiosis, which includes incurable and often fatal coal workers' pneumoconiosis (CWP, or 'black lung'), and silicosis [4] are the most common respiratory disease amongst miners exposed to dust over protracted time periods [NIOSH, 2019]. Such diseases often cause chronic bronchitis and emphysema, and sometimes heart failure and cardiac hypertrophy [Landen et. al., 2011; Brodny and Tutak. 2018]. The particle size fraction $PM_{2.5}$, nominally particulate with an aerodynamic diameter of less than 2.5 microns, which, from urban air pollution studies, has been linked to higher rates of cardiovascular and respiratory mortality [Liu et. al., 2019] is of particular concern. Almost all previous studies were based on PM_{10}.

Symptoms of CWP usually appear after several years, that is why these diseases are most commonly diagnosed in retired miners [Cohen et al., 2018]. Share of new pneumoconiosis cases in Poland caused by coal mining processes is shown in Fig. 1 [Swiatkowska and Hanke, 2018] [Górniczy, 2020]. The persistently high rates of pneumoconiosis suggests that protective measures are insufficient, and/or that dust reduction systems in mines are inadequate.

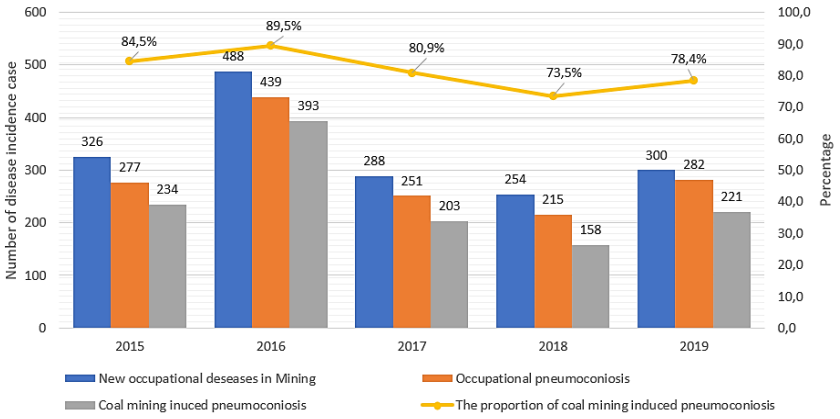

Fig. 1. Share of new pneumoconiosis cases in Poland that are caused by coal mining in the years 2013-2017 [Górniczy, 2020].

Limitation of dust generation decrease of possibility of rising the already settled dust, as well as removing it from air are the main methods for reducing airborne dust concentrations in underground coal mines. Currently, a number of devices and new technologies for dust control using the agents such as: environmentally-friendly agglomerant to improve the dry dust removal effect for filter material for dust removal devices [Liu et al., 2020], or a new ecofriendly crust-dust suppressant extracted from waste paper [Li et al., 2020] are being introduced more and more often. Water spraying is one of the main ways to reduce airborne dust and the likelihood of its resuspension [Ren et al., 2014] [Shi et.al, 2019]. The latter is realized by wetting the settled dust particles, so that they make larger particles and are therefore less likely to be re-suspended. The new high-efficiency coal dust suppressant based on self-healing gel [Ding et al., 2020] limits the effect of dust rising.

Over approximately the last 10 years, a number of spraying devices have been developed for use in hard coal mines. These devices operate by producing a mist of water drops [Wang et al., 2019], each drop potentially captures one or more dust particles. The dust-laden drops have a relatively high mass and are therefore easy to be deposited.

These installations are used on roadheaders [Libera et al. 2010], on longwall shearers [Xu et al. 2019], [Ma et al., 2020], on belt conveyors and in roadways [Bałaga et al., 2015]. All these installations have high dust control efficiency, proved in tests and stand simulations.

One such device, the "water mist generation system with mesh apertures" developed by Telesto's [System, 2020], can operate with use of either water or a mixture of water and compressed air. In both cases special nozzles are used to create water drops with sizes ranging from a few to several tens of micrometres. The device has a spraying frame suspended in the roadway cross-section and a set of movable meshes to catch water-dust droplets.

The CZP BRYZA roadway air-water dust protection system, developed at KOMAG and manufactured by ELEKTRON S.C., is another well-known and commonly used solution for reducing airborne dust [Bałaga et al., 2015] [Prostański, 2018]. The system is equipped with a set of three spraying devices on which the spraying packs (heads) are installed together with linearly arranged spraying nozzles. The nozzles use compressed air which decreases the amount of water required to effectively reduce airborne dust concentration and allows for better water droplet formation. The system operates at water and air pressures of 0.3-0.6 MPa, which restricts its use to the places, where there is access to compressed air and fire-fighting pipelines. In-situ tests of the BRYZA, TELESTO, PNIÓWEK dust protection systems showed that its efficiency for reducing total dust concentration can be as high as 60%, and for PM_{10} around 50% (Fig. 2).

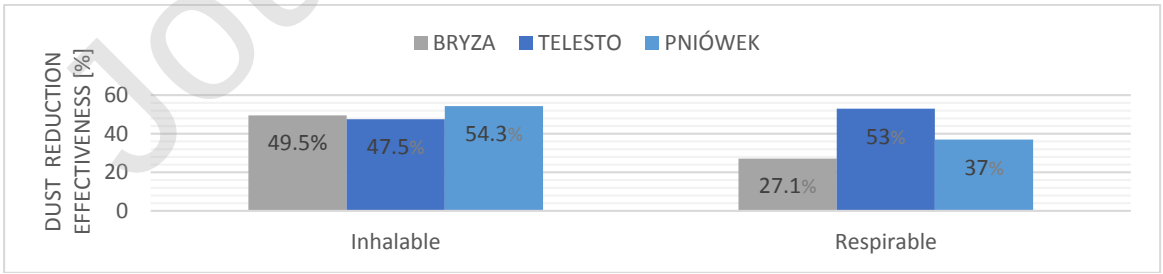

Fig. 2. Efficiency of PM_{10} and PM2.5 dust dust reduction using three tested spraying devices (CZP BRYZA, TELESTO, PNIÓWEK) [Bałaga, 2019]

The air-water spraying solutions presented in Fig. 2 significantly reduce airborne PM_{10} dust levels and so improve the miners safety and work comfort of. It is not known how they reduce PM2.5 dust concentration, as it

was not determined before. Studies on PM 2.5 dust indicate that this fraction causes human diseases, mainly related to the cardiovascular system. The KOMAG Institute has therefore designed a new SSD-1smart spraying device, , which will control both PM_{10} and $PM_{2.5}$ dust [Bałaga, 2019]. The effectiveness of the device will be assessed in underground tests.

2. Theoretical background for the new SSD-1 device

The resuspension of coal dust largely depends on the water content in the dust [Cybulski, 2005], and conversely, dust wetting efficiency is an important factor in removing dust particles from the air . Coal dust will not be resuspended when:

$$W_c > 1.83 x W_{hw} + 2.2 \qquad (1)$$

where:

W_c – total water content in the coal dust, %. It is assumed that W_c has to be at least 8% [Laskowski, 1948] [Cybulski, 2005]

W_{hw} – content of hydroscopic water in coal, %

The three inertial collision, attachment and diffusion mechanisms for combining the dust particles with water droplets are most important to promote their deposition (Fig. 3) [Zacharzewski and Kwiecień, 1974].

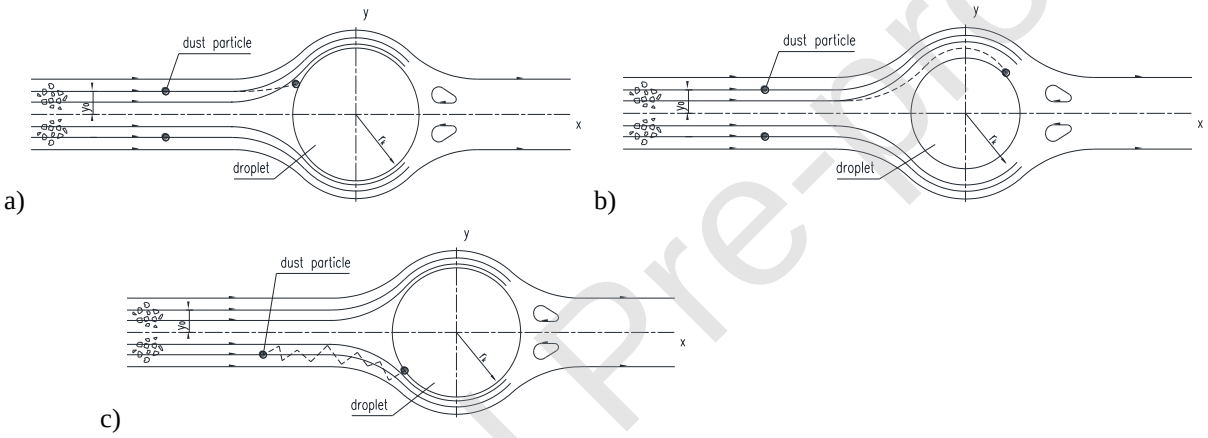

Fig. 3. Mechanisms for combining the dust particle with a water droplet: a) inertia, b) attachment, c) diffusion

The efficiency of dust reduction as a combined effect of inertial collision, attachment and diffusion (Brown's dispersion mechanisms) can be determined from the following relationship [Changchi et al., 1996]:

$$\eta_{ns} = 1 - (1 - \eta_{is})(1 - \eta_{rs})(1 - \eta_{ds}) \qquad (2)$$

where:

η_{ns} effectiveness of dust particle capture by a water droplet, %

η_{is} effectiveness of dust particle capture as a result of inertial collision of a water droplet with a dustparticle, %

η_{rs} effectiveness of dust particle capture as a result of water droplet attachment, %

η_{ds} effectiveness of dust particle capture as a result of water droplet diffusion, %

Efficiency of inertial collision can be calculated from the following relationship given by Herne [Liu et al., 2019]:

$$\eta_{is} = \frac{S_{tk}^{\ 2}}{(S_{tk}+0.25)^2} \qquad (3)$$

$$S_{tk} = \frac{\rho_p d_p^2 v_0}{18 \mu d_c}$$

where:

S_{tk} the inertial collision parameter,

ρ_p the dust density, kg/m^3
d_p the dust particle diameter, m
v_0 the mean relative velocity, m/s

Efficiency of dust particles capturing in the result of attachment with a water drop can be calculated from the following relationship given by Ranz [Liu et al., 2019]:

$$\eta_{rs} = (1 + \frac{d_p}{d_c})^2 - \frac{d_c}{d_c - d_p} \quad (4)$$

where:
d_p the dust particle diameter, m
d_c the droplet diameter, m

Efficiency of dust particles capturing in the result of diffusion in a water drop can be calculated from the following relationship given by Craford [Liu et al., 2019]:

$$\eta_{ds} = 4.18\, Re_d^{\frac{1}{6}} Pe^{-\frac{2}{3}} \quad (5)$$

$$Re_d = \frac{v_0\, d_c \rho_g}{\mu} \quad (6)$$

$$Pe = \frac{v_0\, d_c}{\mu} \quad (7)$$

where:
Re_d the Reynolds number,
Pe the Peclet number,
d_c the droplet diameter, m
v_0 the mean relative velocity, m/s
ρ_g the air density, kg/m^3
μ the air dynamic viscosity, Pa*s

According to tests carried out by Karowiec [Karowiec, 1984], the efficiency of water droplets to capture dust particles depends on their size and energy. It decreases rapidly as the diameter of dust particles decreases, and increases with reduction in water droplet diameter. Unfortunately, a reduction in water droplet diameter, and an increase in the distance from the spraying nozzle, can cause a loss of water drop energy, which leads to a decrease in the efficiency of dust deposition. Karowiec's tests were carried out for dust particles smaller than 5 μm (Fig. 4).

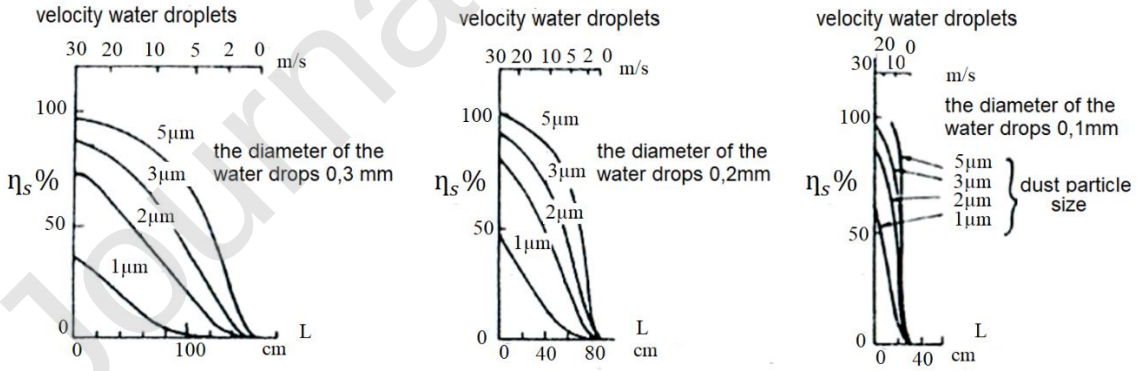

Fig. 4. Efficiency of dust particle capture by water droplets of different diameters, which depends on the size of the dust particle and distance from the spraying source [Karowiec, 1984].

Producing smaller diameter droplets increases their total surface area compared with larger droplets from the same volume of water, which contributes to increasing the efficiency of dust particle capture [Lebecki et al., 2004]. The following calculations confirm this:

V_r - *volume of droplet of radius* r,
$V_{0,1r}$ - *volume of droplet of radius* 0.1r.

$$V_r = \frac{4}{3}\pi r^3 \quad (8)$$

$$V_{0,1r} = \frac{4}{3}\pi\left(\frac{1}{10}r\right)^3 = \frac{1}{1000} \times \frac{4}{3}\pi r^3 = \frac{1}{1000}V_r \quad (9)$$

Assuming that droplet radius is reduced by 10 times, the surface area of the droplets will be:

$$S_r = 4\pi r^2 \quad (10)$$

$$S_{0,1r} = 4\pi\left(\frac{1}{10}r\right)^2 = \frac{1}{100} \times 4\pi r^2 = \frac{1}{100}S_r$$

$$S_{1000} = 100 \times 4\pi\left(\frac{1}{10}r\right)^2 = \frac{1}{100}r^2 \times 1000 \times 4\pi = 10 \times 4\pi r^2 = 10S_1$$

Where S_{1000} is the surface of 1000 drops of radius $r = \frac{1}{10}r$, and their volume corresponds to 1 droplet with a radius r.

From these calculations, a 10-fold reduction in the radius of the droplets causes their total surface area to increase by 10 times, which increases the probability of a water droplet encountering a dust particle. At the same speed, however, smaller diameter water droplets have lower kinetic energy, which worsens their effectiveness for capturing dust particles. To overcome this, the velocity of droplets can be increased by using a high pressure water system to supply the spraying nozzles. Unfortunately, such systems require special pumps which generate additional costs. Using compressed air can produce smaller diameter droplets with relatively high kinetic energy [Siegmund et al., 2018] [Wang et al., 2019].

3. SSD-1Smart Spraying Device

Currently used spraying devices produce droplets of unknown sizes and velocity and do not respond to changing dust concentration. With knowledge of the theoretical background, and having experience from several hundred installations of spraying devices [Bałaga et al., 2015] [Prostański, 2018], a team of KOMAG designers has developed a new smart SSD-1spraying device, the, for use in roadways [Bałaga, 2019]. The operational principle of the device is to produce water droplets with diameters close to the size of the dust particles, and to maintain a high output energy from the nozzles by using water combined with compressed air (Fig. 5) [Wang et al., 2019].

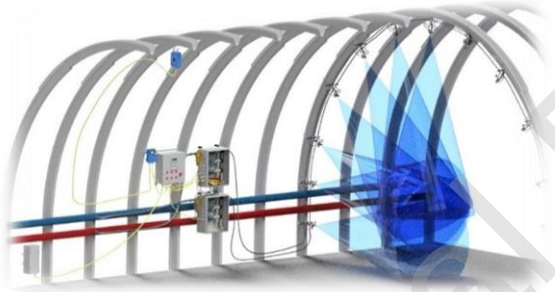

Fig. 5. 3D visualisation of the new SSD-1 smart spraying system [Bałaga, 2019]

The prototype of the SSD-1 device has several spraying units installed on the perimeter of the roadway support, to which water and compressed air are supplied from special units. Both water and compressed air flow through one of the three supply lines, within which the pressure is adjusted by reduction valves. The SSD-1 device creates spraying streams with different droplets fractional distributions, produced and controlled by nine water and compressed air pressure combinations. From the measurement of ambient PM_{10} and $PM_{2.5}$ dust concentrations, using an EMIDUST optical dust meter, the MDJ6001 intrinsically safe controller uses an algorithm to select the optimum water and compressed air pressures. Photographs of the functional testing of the prototype device are shown in Fig. 6.

Fig. 6. Functional tests of the SSD-1 smart spraying device.

4. Droplet fractional distribution tests

For the correct operation of the SSD-1 device and its control algorithm, it was necessary to develop and manufacture a prototype nozzle. This was tested using a test stand, built at the KOMAG Institute of Mining Technology, which consisted of a nozzle supplied with water and compressed air, instruments for recording the spraying parameters and a Spraytec droplet analyser made by Malvern Instruments (Fig. 7). The water spraying stream was tested at a distance of 1 m from the nozzle end. The aim was to determine the fractional distribution of droplets which depends on water and air supply pressures. Based on the results, the best water nozzle supply parameters were selected for the most efficient and effective reductions in PM_{10} and $PM_{2.5}$.

Fig. 7. Test stand used for the measurement of water droplets fractional distribution in the spray stream, where the source of the spraying stream was located at a distance of 1 m from the Spraytec droplets analyser.

Fractional droplets distribution tests in the spraying streams generated by nozzles supplied with water and compressed air were carried out according to the combinations of parameters listed in Table 1. These parameters resulted from the range of proper operation of the nozzle and parameters of media available in mine underground.

Table. 1. Water and compressed air pressures and corresponding combination numbers

Pressure/Combination No.	1	2	3	4	5	6	7	8	9	10	11	12	13	14	15	16
P_{water} *[MPa]*	0.05	0.05	0.05	0.05	0.1	0.1	0.1	0.1	0.2	0.2	0.2	0.2	0.3	0.3	0.3	0.3
P_{air} *[MPa]*	0.2	0.3	0.4	0.5	0.2	0.3	0.4	0.5	0.2	0.3	0.4	0.5	0.2	0.3	0.4	0.5

After stabilization of the spraying stream and water and air outputs, the results of the droplet distribution tests were recorded. The spray streams supplied by different combinations of water pressure and compressed air are shown in Fig. 8.

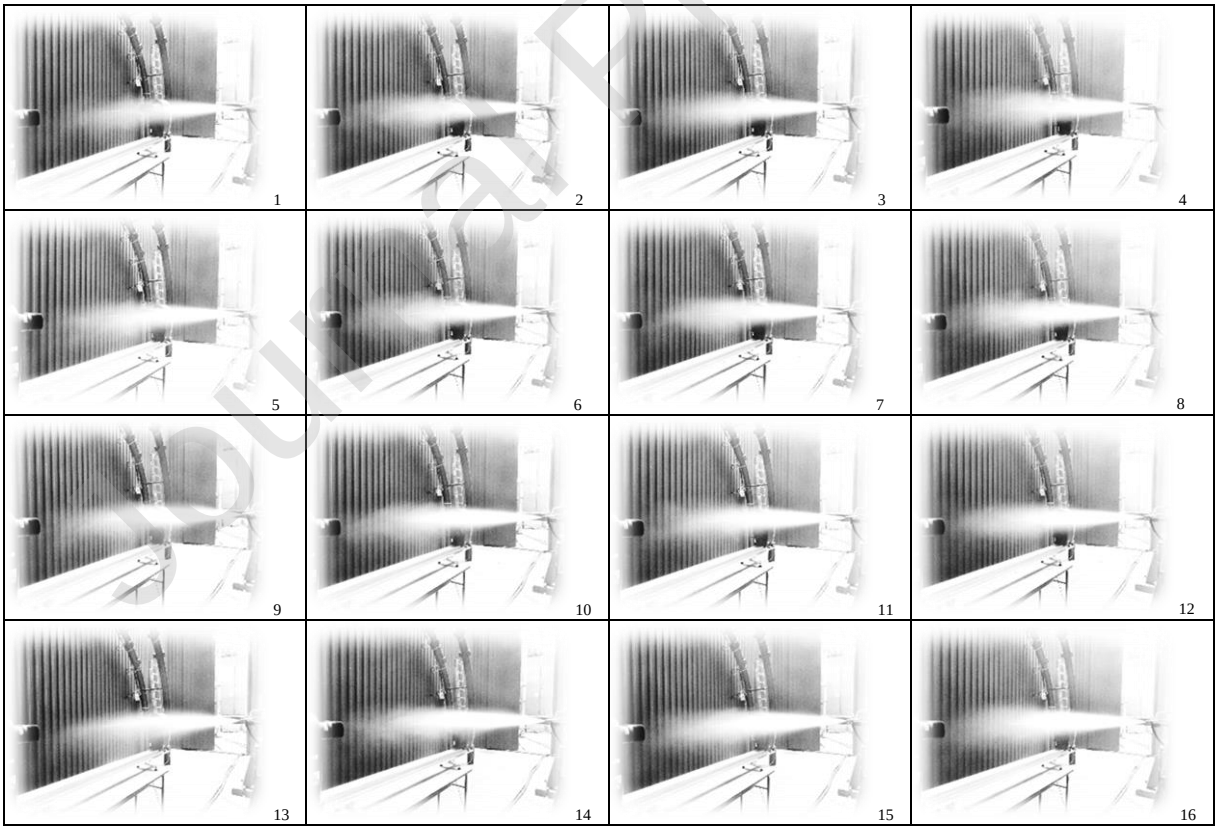

Fig. 8. Spraying streams generated by the nozzle when supplied with water and compressed air at given combinations of water and compressed air pressures

5. Droplet fractional analysis

The results obtained from the tests were for the percentage share of droplets, the D32 Sauter mean diameter and the cumulative curve. The dust capture effectiveness of the generated water stream produced at each of the tested combinations of water nozzle supply parameters was assessed. Firstly, based on the result of the D32 Sauter mean diameter and the flowrate of water supplying the spraying nozzle, the total surface area of generated drops was calculated. This assumed that the droplets had the shape of an ideal sphere, which surface area and volume were calculated using the following formula:

$$P_k = 4\pi \cdot r^3 \quad (11)$$

where:

P_k - the single drop surface area, m^2

r - the drop radius (0.5 D32 Sauter diameter), m

In turn, the volume of the droplets was calculated from the following formula:

$$\boldsymbol{V_k = \frac{4}{3}\pi \cdot r^3} \quad (12)$$

where:

V_k - the single droplet volume, m^3

r - the droplet radius (0.5 D32 Sauter diameter), m

Knowing the volumetric flowrate of the water supplying the Q_w nozzle, and the volume of a single droplet (determined using the Sauter mean diameter), it was possible to calculate the mean number of all droplets in the spraying stream, generated per minute. The number of drops n_t is calculated from the following formula:

$$\boldsymbol{n_t = \frac{Q_w}{V_k}} \quad (13)$$

where:

n_t - equivalent number of drops generated in 1 min,

Q_w - water flow rate, $\frac{m^3}{min}$,

V_k - single drop volume, m^3.

The total absorption surface area generated by the nozzle in 1 minute was calculated using the following formula:

$$PA/T = n_t \cdot P_k \quad (14)$$

where:

PA/T - absorption surface area created within 1 min, m^2

n_t - equivalent number of drops generated within 1 min

P_k - single drop surface area, m^2

Thus, the determined absorption surface areas generated within 1 min, for the spraying streams [Bałaga et al., 2019], at given combinations of water and compressed air pressures, are presented in Table 2.

Table. 2. Droplet diameter and absorption surface area for the different combinations of water and compressed air flow rate

Combination number	***Water flow rate [dm³/min]***	***Air flow rate [Ndm³/min]***	***Diameter D(32) [µm]***	***PA/T [m²/min]***
1	*0.24*	*18.83*	*61.25*	*23.5*
2	*0.22*	*25.98*	*49.51*	*26.7*
3	*0.18*	*32.2*	*37.13*	*29.1*
4	*0.17*	*35.99*	*31.82*	*32.1*
5	*0.38*	*16.37*	*77.34*	*29.5*
6	*0.34*	*25.51*	*62.69*	*32.5*
7	*0.3*	*31.68*	*50.34*	*35.8*
8	*0.28*	*35.43*	*43.82*	*38.3*
9	*0.62*	*12.28*	*96.66*	*38.5*
10	*0.53*	*23.26*	*69.23*	*45.9*
11	*0.54*	*31.15*	*61.98*	*52.3*
12	*0.49*	*35.16*	*58.34*	*50.4*
13	*0.99*	*6.14*	*142*	*41.8*
14	*0.73*	*16.77*	*83.41*	*52.5*
15	*0.74*	*28.51*	*69.62*	*63.8*
16	*0.67*	*32.67*	*65.97*	*60.9*

It is possible to obtain different sizes of water droplets in the spraying stream by changing the pressure of the water and compressed air supplying the nozzle. The results are presented in a graphical form in Fig. 9. The smallest D32 Sauter mean diameter,of 31.82 µm, was measured at the lowest water pressure and the highest compressed air pressure. In turn, the highest D32 Sauter mean diameter of 142 µm was measured at the highest water pressure and the lowest compressed air pressure., Increase in air and water pressure, at the same flow rate, decreases a droplet diameter. In turn, a decrease in the difference between the water and relative air pressure increases the D32 Sauter mean droplet diameter.

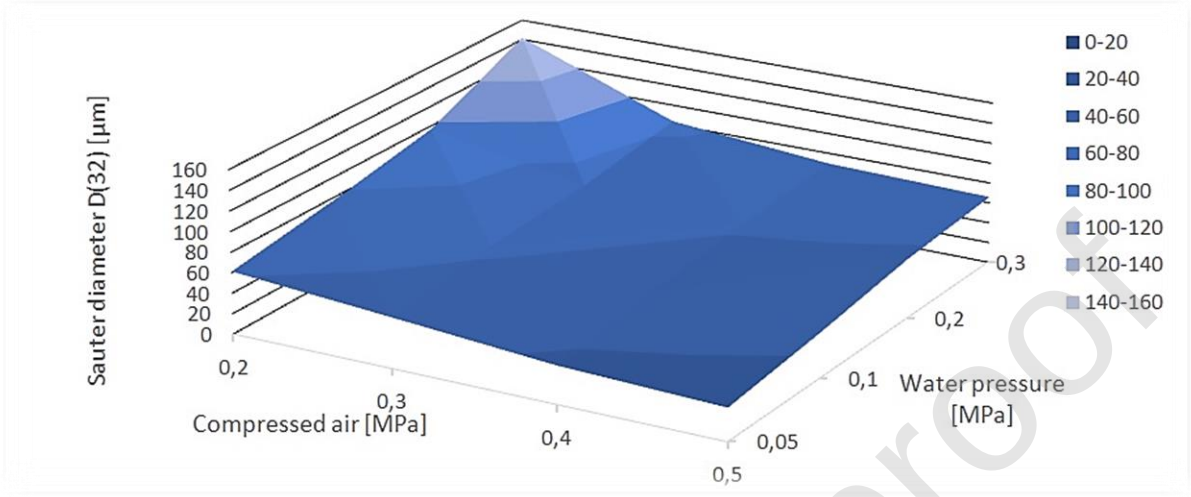

Fig. 9. The D32 Sauter mean droplet diameter which depends on the pressure of water and compressed air supplying the nozzle

The situation is different for the absorbtion surface area (Fig. 10) where the highest values were obtained at the highest water and compressed air pressures (0.4 MPa air and 0.3 MPa water), and the lowest at the lowest water and compressed air pressures (0.2 MPa air and 0.05 MPa water). The highest absorption surface area was about 64 m^2/min, and the lowest around 24 m^2/min.

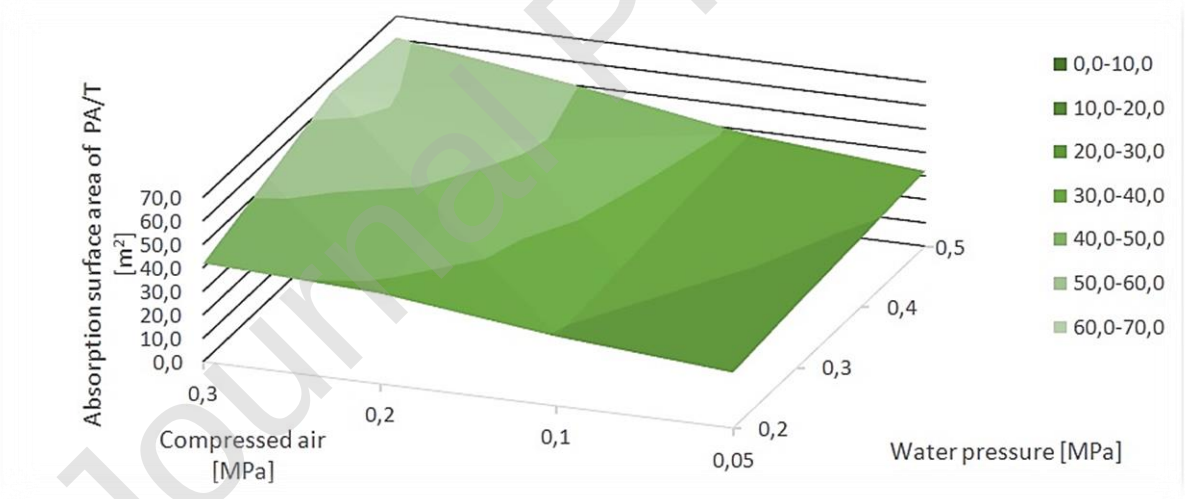

Fig. 10. Absorption surface area of PA/T droplets, which depends on the pressure of water and compressed air supplied to the nozzle.

The tests also indicated that the size of the absorption surface area and the diameter of the droplets in the tested two-media nozzle, with external mixing, is controlled by the amount of water and compressed air supplied to the nozzle. The increase in water flowrate is directly proportional to the increase in its pressure and inversely proportional to the decrease in compressed air pressure (Fig. 11).

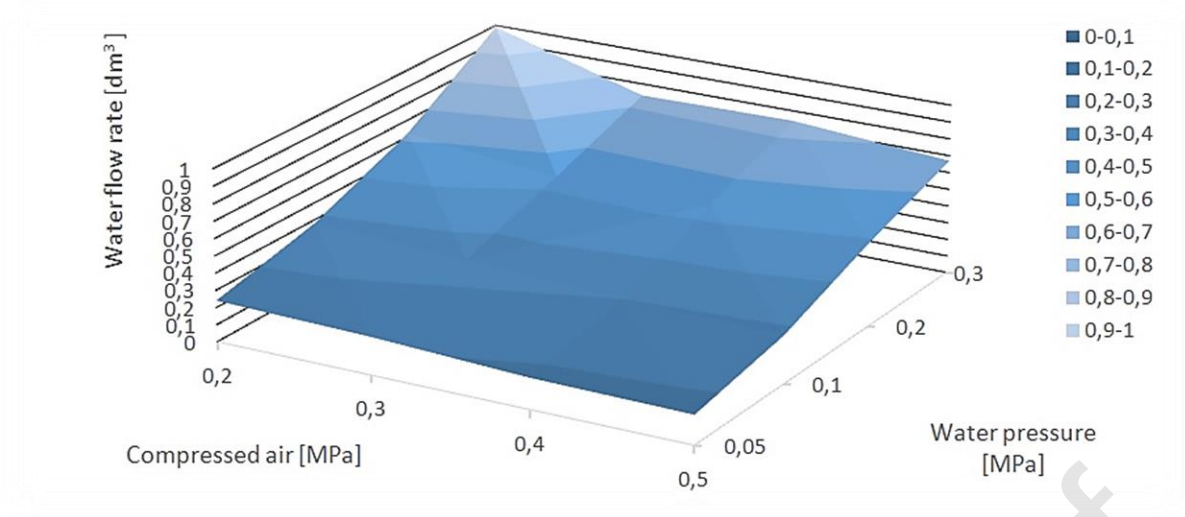

Fig. 11. Water flow rate [dm³/min], which depends on the pressure of water and compressed air supplied to the nozzle.

A similar effect is observed for air flow rate. An increase in air flow rate is directly proportional to the increase in air pressure and inversely proportional to the increase in water pressure (Fig. 12).

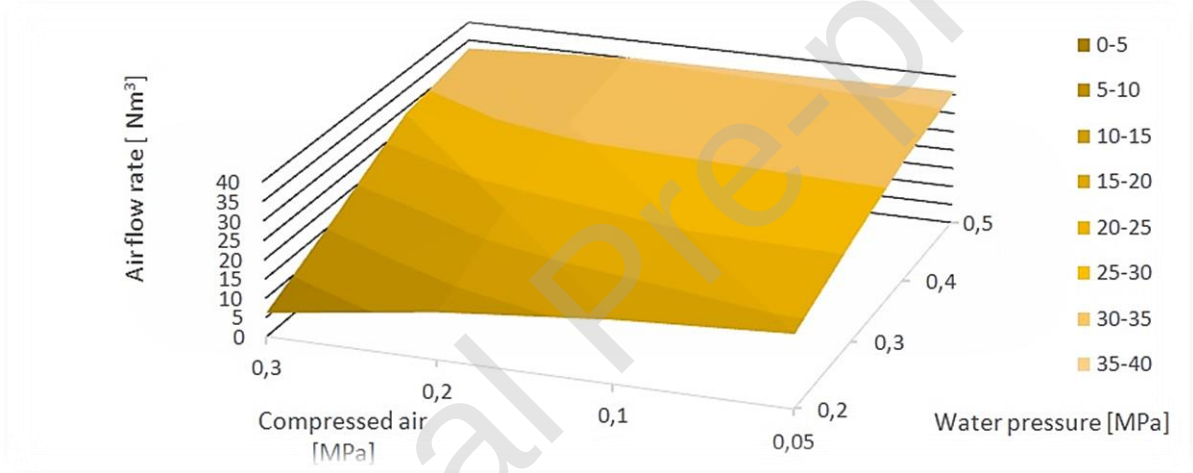

Fig. 12. Air flow rate [Ndm³/min], depending on the water pressure and compressed air supplied to the nozzle

For such tests on the effects of different nozzle parameters on droplet characteristics, the energy needed to produce the air-water spray stream was additionally determined. This energy is a sum of energy needed to produce the required air flow rate, and the pressure needed to generate the required water flow rate and pressure, within a given time [Rojek and Kalukiewicz, 2012].

$$E = E_P + E_W \quad (15)$$

The energy required to generate the given air parameters is the following:

$$E_P = \dot{V}_P \cdot p_P \cdot \tau \quad (16)$$

where:

$\dot{V}_P$ - air volume over a given time interval[m³]
p_P - air pressure [Pa]
τ - time [min]

By treating air as an ideal gas, we can write:

$$\dot{V}_{PN} \cdot p_{PN} = n \cdot R \cdot T_{PN} \quad (17)$$

where:

$\dot{V}_{PN}$ - air volume under normal conditions over a given time interval, Nm^3
p_{PN} - air pressure under normal conditions ($p_{PN} = 101325$ [Pa])
n - number of air moles
R - individual gas constant of air ($R = 287$ $\frac{J}{kgK}$)
T_{PN} - air temperature under normal conditions ($T_{PN} = 273.15,$ K)

As the results for the air flow rate are related to normal conditions, they should be converted into real conditions in the pipe supplying the nozzle:

$$\dot{V}_P \cdot p_P = n \cdot R \cdot T_P \quad (18)$$

where:

$\dot{V}_P$ - air volume over a given time interval, m^3
p_P - air pressure under real conditions
n - number of air moles
R - individual gas constant of air ($R = 287 \frac{J}{kgK}$)
T_P - air temperature in real conditions ($T_P = 288.35,$ K)

After comparison of equations (18) and (19) we get:

$$\dot{V}_P = \frac{\dot{V}_{PN} \cdot T_P \cdot p_{PN}}{T_{PN} \cdot p_P} \quad (19)$$

In turn, the energy required to generate the given water parameters is the following:

$$E_W = \dot{V}_W \cdot p_W \cdot \tau \quad (20)$$

The determined energy consumption is presented in Table. 3.

Table. 3. Energy consumption required to obtain each combination of parameters to provide different spray streams.

Combination number	***Water flow rate [dm³/min]***	***Air flow rate (normal conditions) [Ndm³/min]***	***Air flow (real conditions) [m³/min]***	***Air energy E_p [kJ]***	***Water energy E_w [kJ]***	***Energy E [kJ]***
1	*0.24*	*18.83*	*0.0100*	*2.01*	*0.01*	*2.03*
2	*0.22*	*25.98*	*0.0093*	*2.78*	*0.01*	*2.79*
3	*0.18*	*32.2*	*0.0085*	*3.39*	*0.01*	*3.4*
4	*0.17*	*35.99*	*0.0077*	*3.85*	*0.01*	*3.86*
5	*0.38*	*16.37*	*0.0087*	*1.75*	*0.04*	*1.79*
6	*0.34*	*25.51*	*0.0091*	*2.73*	*0.03*	*2.76*
7	*0.3*	*31.68*	*0.0083*	*3.33*	*0.03*	*3.36*
8	*0.28*	*35.43*	*0.0076*	*3.79*	*0.03*	*3.82*
9	*0.62*	*12.28*	*0.0065*	*1.31*	*0.12*	*1.44*
10	*0.53*	*23.26*	*0.0083*	*2.49*	*0.11*	*2.59*
11	*0.54*	*31.15*	*0.0045*	*1.79*	*0.11*	*1.9*
12	*0.49*	*35.16*	*0.0075*	*3.76*	*0.10*	*3.86*
13	*0.99*	*6.14*	*0.0033*	*0.66*	*0.30*	*0.95*
14	*0.73*	*16.77*	*0.0115*	*3.44*	*0.22*	*3.66*
15	*0.74*	*28.51*	*0.0076*	*3.05*	*0.22*	*3.27*
16	*0.67*	*32.67*	*0.0070*	*3.49*	*0.20*	*3.7*

Water and air energy required to generate 1 m^2 of absorption surface depends on the combination of air-water nozzle supply parameters, as shown in Fig. 13.

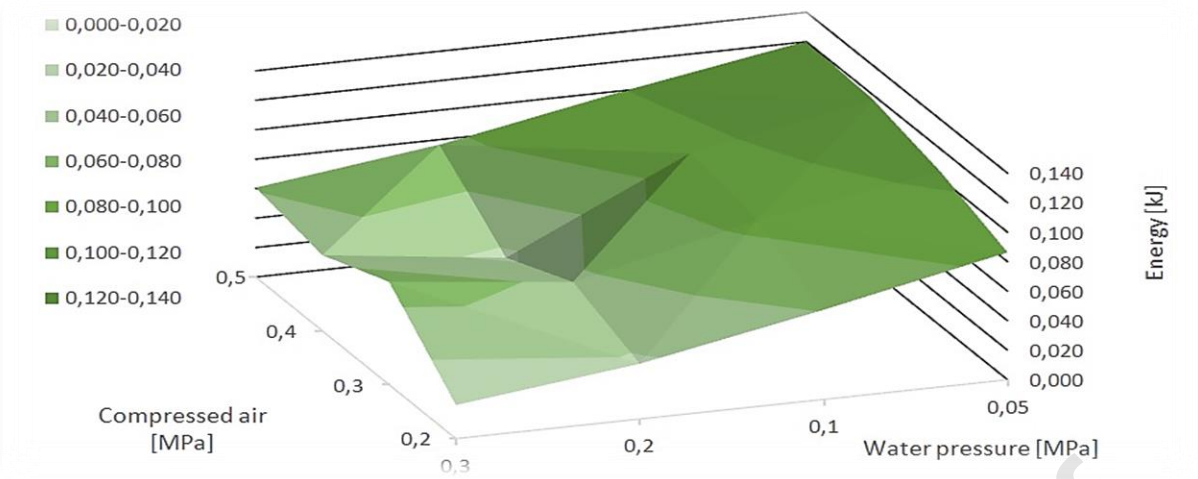

Fig. 13. Water and compressed air energy consumption to generate a 1m^2 absorption surface, which depends on the relative pressures of water and compressed air supplied to the nozzle

From the energy needed to generate a given droplet distribution, the least preferable setting is a water pressure below 0.1 MPa, where the energy required for a 1m^2 absorption area is above 0.1 kJ. The most favourable water supply pressure is above 0.1 MPa, where the required energy is only 0.23 kJ/m^2 (0.3 MPa water and 0.2 MPa air). Unfortunately, this case is the least favourable in terms of the D32 Sauter mean diameter.

6. Selection of optimum combination of water spraying stream parameters to the given dust concentration

After fractional analysis of the spraying stream, the optimum combination of parameters were selected to reduce airborne dust concentrations using the SSD-1 smart spraying device. As the device has 3 possible settings for water pressure, and 3 for compressed air pressure, there are nine combinations of air and water pressures. The optimum parameters were selected over a number of test stages.

At the first stage, the pressure reducer settings in the spraying device were determined, taking into account the energy demand needed to generate a 1 m^2 absorption surface area. Due to the large amount of energy required, water pressures below 0.1 MPa, were rejected. Waterpressures of 0.1 MPa, 0.2 MPa and 0.3 MPa were selected for the reducer settings, in combination with compressed air pressures equal to 0.3 MPa, 0.4 MPa and 0.5 MPa. The lowest compressed air pressure was combined with the highest water pressure of 0.3 MPa to give better droplet distribution. Cumulative curves for the selected combinations of the spray nozzle parameters are presented in Fig. 14.

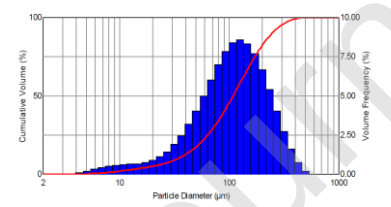

6. *(P_w-0.1 MPa, P_p-0.3MPa)*

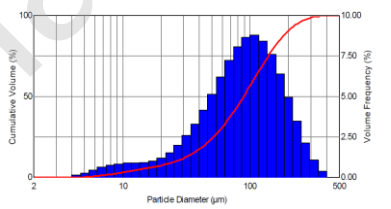

7. *(P_w-0.1 MPa, P_p-0.4MPa)*

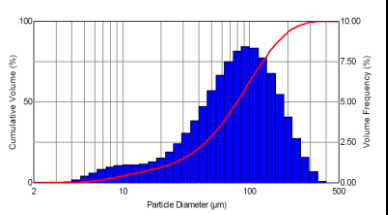

8. *(P_w-0.1 MPa, P_p-0.5MPa)*

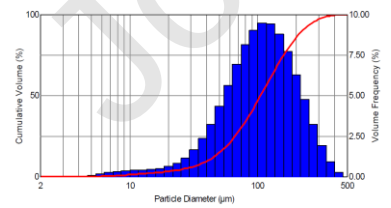

10. *(P_w-0.2 MPa, P_p-0.3MPa)*

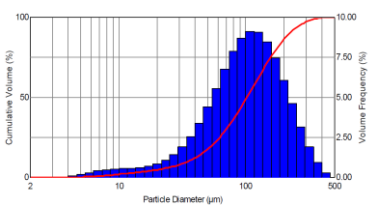

11. *(P_w-0.2 MPa, P_p-0.4MPa*

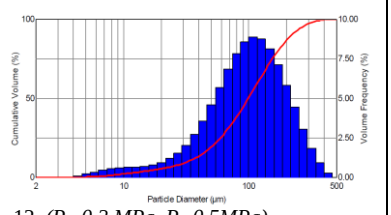

12. *(P_w-0.2 MPa, P_p-0.5MPa)*

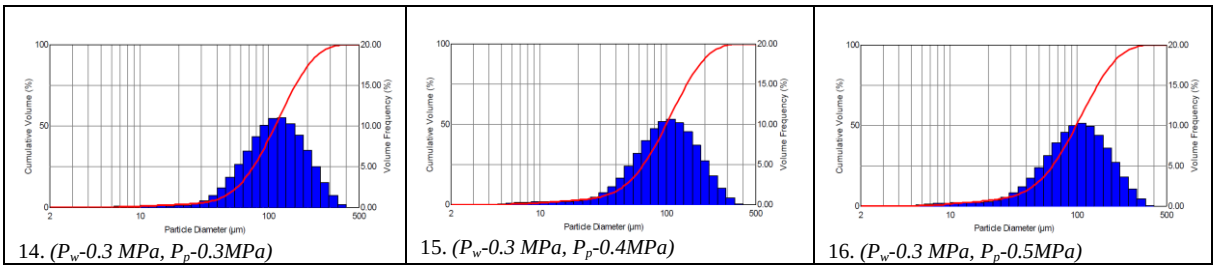

14. *(P_w-0.3 MPa, P_p-0.3MPa)* 15. *(P_w-0.3 MPa, P_p-0.4MPa)* 16. *(P_w-0.3 MPa, P_p-0.5MPa)*

Fig. 14. Cumulative curves of droplet diameter achieved by the selected combinations of spray stream parameters.

The next step was to determine which of the 9 combinations of water pressure and compressed air settings, in terms of absorption surface and the mean diameter of the droplets they produce (Sauter mean diameter), would be best for capturing the PM_{10} and $PM_{2.5}$, measured using the EMIDUST continuous dust monitoring system. (Table 2). Based on gained experience [Bałaga and Jaszczuk, 2016], in controlling the PM_{10} dust, the largest absorption surface generated by the spraying streams should be used. In turn, from the highest absorption surfaces for effective control of $PM_{2.5}$ dust, the smallest mean diameter should be selected. On this basis, a SSD-1 spraying device response to dust fractional analysis table was created (Table. *4*).

Table. 4. Table of response for SSD-1 smart spraying device (number of combination.)

Number of combination		*Concentration of PM_{10}*		
		<20 mg/m³	*20-40 mg/m³*	*>40 mg/m³*
Concentration of $PM_{2.5}$	*<10 mg/m³*	*8*	*12*	*16*
	10-50 mg/m³	*7*	*11*	*15*
	>50 mg/m³	*6*	*10*	*14*

The smart SSD-1 spraying device was programmed for using the numbers of media pressure combination depending on dust concentration and composition given in Table 4, and then its operation was verified in operational tests at KOMAG. As part of this, the dust concentration was manually entered into the MDJ controller's software and the nature of the response of the spray system to PM_{10} and $PM_{2.5}$ dust concentrations was assessed, especially the time required for valve activation and thus the initiation of the spraying system.

Each of the assessed spray nozzle supply combinations differed significantly in the characteristics (range and intensity) of the droplet stream produced by the nozzle. Fig. 15 illustrates the effect of different water and compressed air pressures combination on the spraying stream characteristics produced by the SSD-1 device.

6. (P_w-0.1 MPa. P_p-0.3MPa) 7. (P_w-0.1 MPa. P_p-0.4MPa) 8. (P_w-0.1 MPa. P_p-0.5MPa)

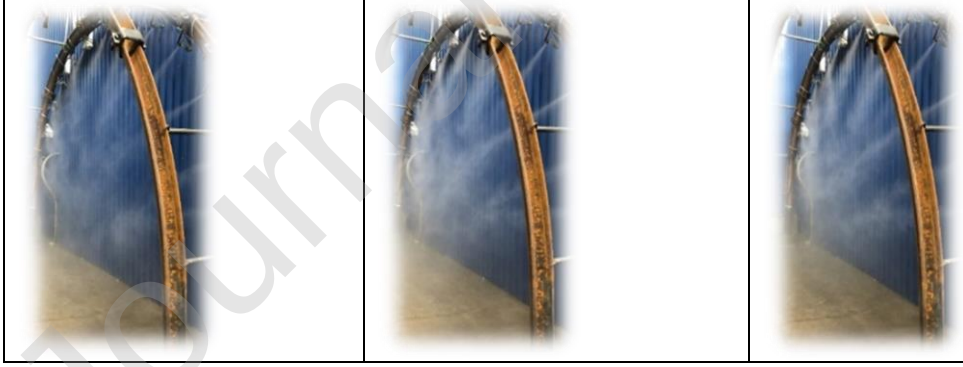

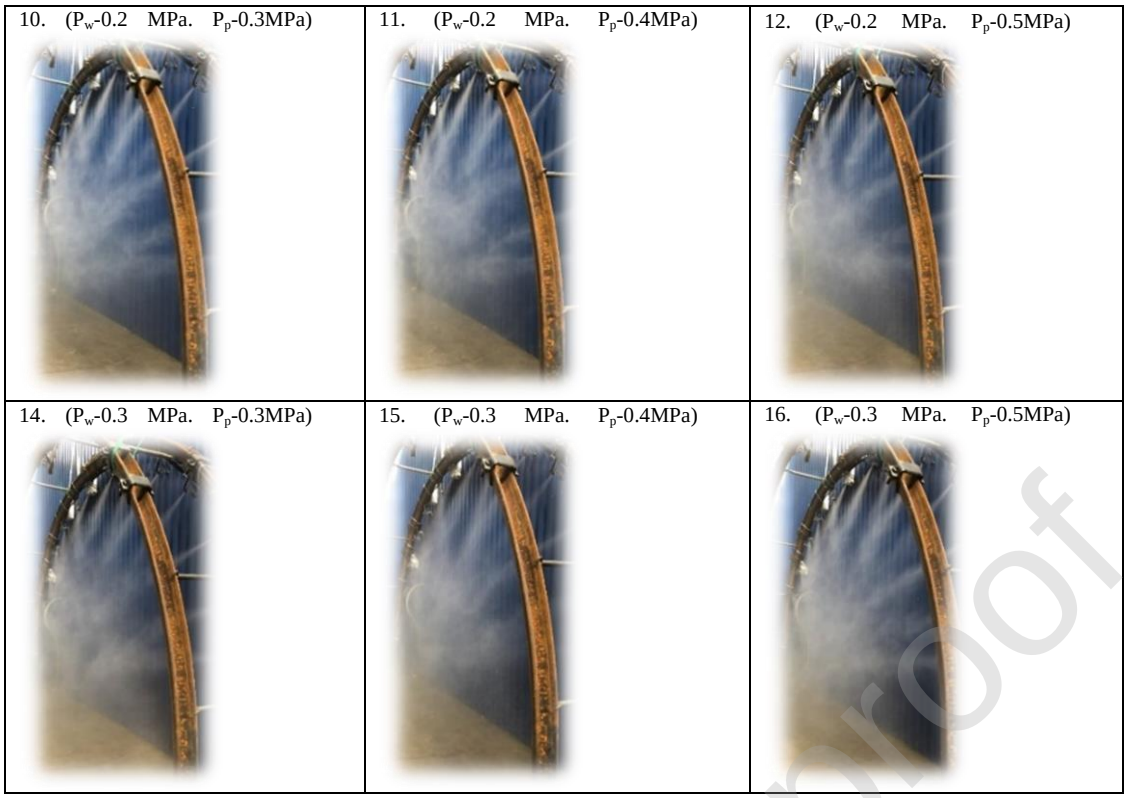

Fig. 15. Production of water mist curtain in a simulated mine roadway cross-section which depends on the size distribution of droplets produced at different pressures of water and compressed air (ultimately chosen combinations)

7. Underground in-situ tests

After positive operational verification tests of SSD-1 smart spraying device in the testing room, it was transported to KWK Pniówek mine. SSD-1 device was installed in N-3 in the seam 404'4. Testing its effectiveness in controlling PM10 and PM2.5 dust concentration and comparing the results with those reported in the case of currently used spraying devices was the main objective of the underground tests (Fig. 16). Measurements of PM10 and PM2.5 dust concentration were measured, as in the case of currently used devices, by the personal gravimetric dust meters type CIP-10R for measurements of PM2.5 dust fraction and type CIP-10I for PM10 fraction. Dust concertation measurements were taken ahead of the spraying device and behind it (at a distance of about 20m) for each of nine combinations of spraying stream parameters.

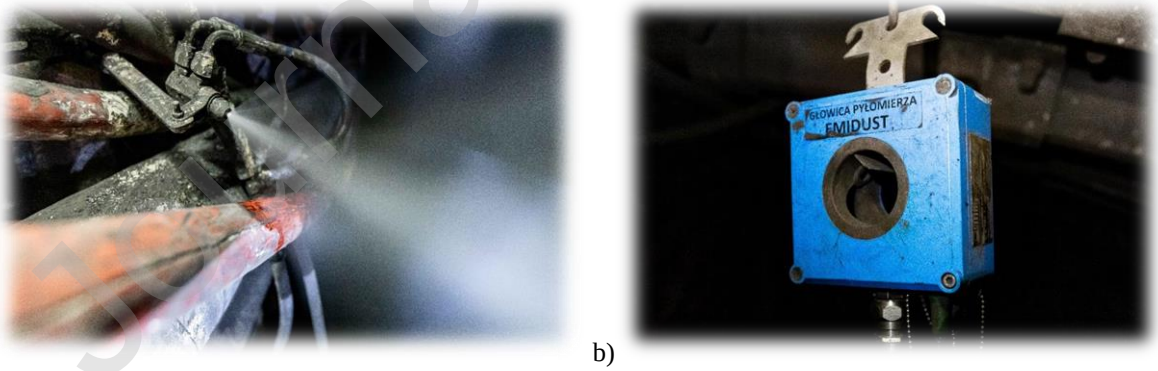

a) b)

Fig. 16. View of: a) the two-media nozzle of the SSD-1 device in operation, b) the EMIDUST's measuring head.

The results of the CIP-10R and CIP-10I particle counter measurements allowed to calculate the average dust concentration at given measuring points. The following formula for determination of dust concentration in the air was used (21).

$$\overline{S} = \frac{m}{V * \tau} \qquad (21)$$

where:

$\overline{S_1}$ – measured dust concentration $[\frac{mg}{m^3}]$

$V - airflow\ in\ CIP - 10\ [\frac{dm^3}{min}]$

$\tau - measurement\ time\ [\ min]$

$m - mass\ of\ \ dust\ in\ the\ measuring\ cup\ \ [mg]$

Results of average concentrations of PM10 and PM2.5 dust, measured around the tested device, allowed to calculate the tested spraying device efficiency in dust reduction . This efficiency was calculated according to the formula (22). Efficiency of PM10/PM2.5 dust reduction is the difference between the PM10/PM2.5 dust concentration measured ahead of the spraying device and the PM10/PM2.5 dust concentration measured behind the spraying device.

$$\eta_{red\ zap} = \frac{\overline{S_1} - \overline{S_2}}{\overline{S_1}} x100\% \qquad (22)$$

where:

$\overline{S_1}$ – dust concentration ahead of the spraying device

$\overline{S_2}$ – dust concentration behind the spraying device

The measuring cycle consisting in dust concentration measurements for nine combinations of spraying parameters was completed within one working shift. During two following days, additional two measuring cycles were made .

Underground tests for determination of efficiency in reduction of PM2.5 and PM10 dust concentration by the smart spraying device enabled to find clear relationships between spraying stream parameters and dust concentration. Based on the results of PM10 dust reduction efficiency, it was observed in each of three measuring days, that the efficiency increased with water pressure increase. It was also observed that in all testing days dust reduction efficiency increased when difference of water pressure and compressed air pressure was small (0.1MPa water and 0.3 MPa compressed air- combination No. 6; 0.2MPa water and 0.3 MPa compressed air- combination No. 10 ; 0.3MPa water and 0.3 MPa compressed air- combination No. 14) Fig. 17.

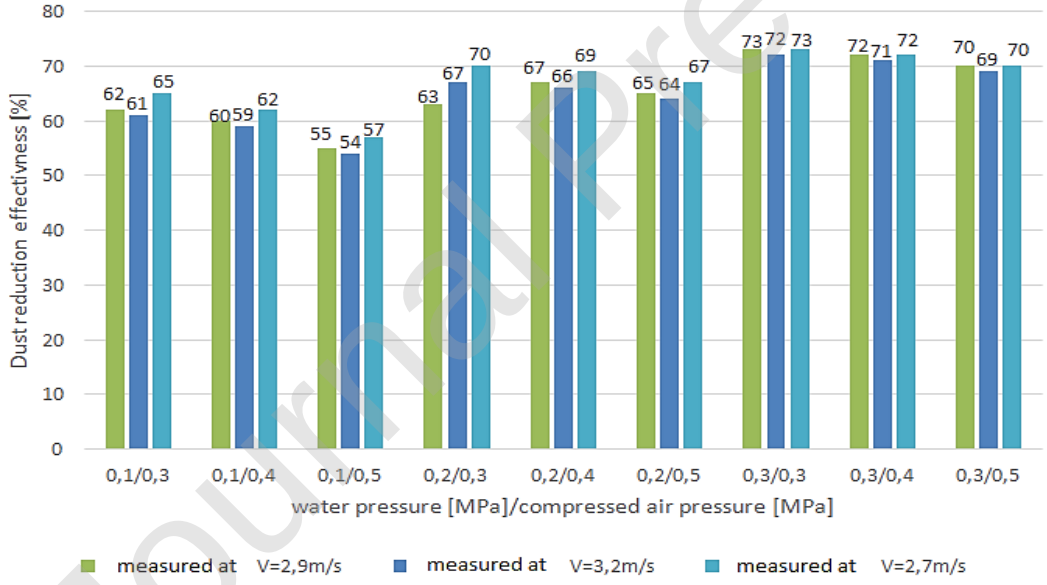

Fig. 17. Effectiveness in reduction of PM10 dust concentration depending on pressure of water and compressed air supplying the spraying nozzles in relation to air flowrate measured in a roadway

During three measuring days, air flowrate was measured using the anemometer. The recorded flowrates were successively: 2.9m/s; 3.2 m/s and 2.7 m/s. Impact of air flowrate on efficiency of PM10 and PM2.5 dust was observed, where the highest dust reduction efficiency was found for the lowest air flowrate equal to 2.7 m/s.

Based on the results of efficiency in reduction of PM2.5 dust, obtained in each of three measuring days, it was observed that this efficiency reduced with increase of water pressure . It was also observed that in all testing days PM2.5 dust reduction efficiency increased when difference of water pressure and compressed air pressure was high (0.1MPa water and 0.5 MPa compressed air - combination No. 8; 0.2 MPa water and 0.5 MPa compressed air - combination No. 12 ; 0.3MPa water and 0.5 MPa compressed air - combination No. 16). Fig. 18

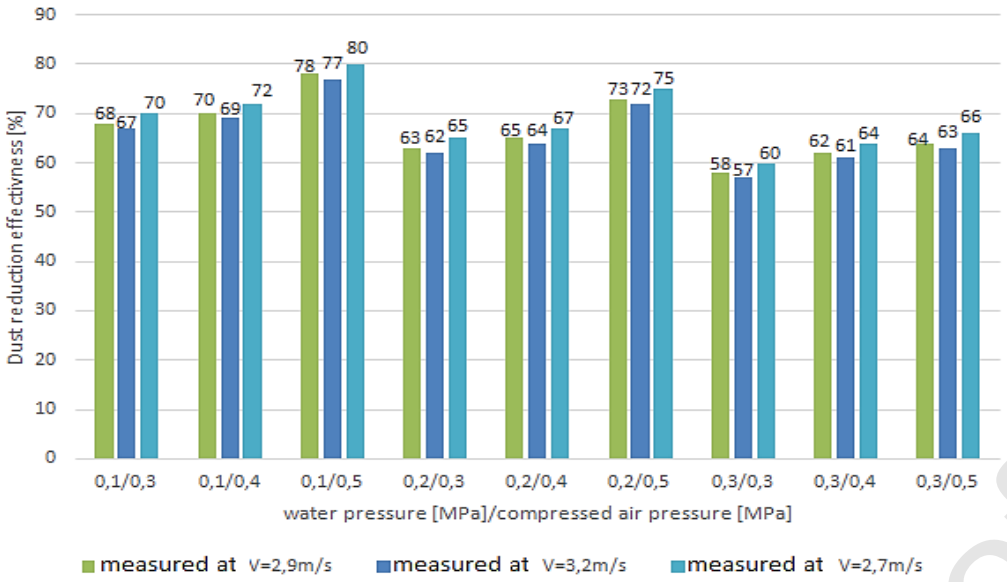

Fig. 18. Effectiveness in reduction of PM2.5 dust concentration depending on pressure of water and compressed air supplying the spraying nozzles in relation to air flowrate measured in a roadway

Average concentrations of PM10 and PM2.5 dust ahead and behind the SSD-1 spraying device obtained during three days of measurements were compared with the results obtained for the currently used spraying devices, Fig. 19.

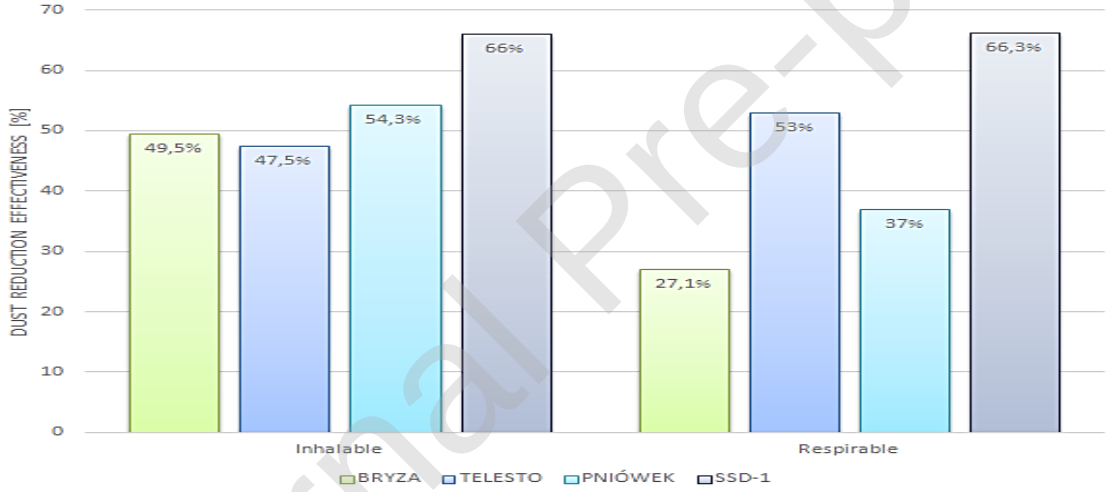

Fig. 19. Comparison of dust control efficiency of currently used and SSD-1 spraying devices

8. Conclusions

High airborne dust concentrations in underground hard coal mines in Poland need to be mitigated urgently to reduce the risks from explosions and to the respiratory health of mine workers. From previous studies [Ren et al., 2014; Shi et al., 2005; Wang et al., 2019], it was suggested that future dust suppression systems should be based on water driven by compressed air to produce droplet spray streams and curtains [Wang et al., 2019; System, 2020; Bałaga et al., 2015; Prostański, 2018; Bałaga, 2019]. To address this, KOMAG has recently prototyped an smart spraying device, SSD-1, which is designed to optimise the size and concentration of water droplets to match those of ambient dust particles, the latter continuously measured using an EMIDUST monitoring device. From an analysis of droplet size distribution and absorption surface area in the spray stream, water droplets of different sizes can be produced by varying the pressure of supplied water and compressed air. The prototype of the SSD-1 smart spraying device has been subject to functional tests, during which its operational capabilities and the speed of response to changing dust concentrations were found to be excellent.

After functional tests, the SSD-1 device was installed in the Pniówek coal mine, where it was tested for the reduction of PM10 and PM2.5 dust. The presented results of the efficiency of PM2.5 dust reduction are consistent

with the determined Sauter mean diameters (D32), where the smallest diameters were obtained in the case of an increased difference between compressed air pressure and water pressure. In addition, the increase in water and compressed air pressure caused an increase in the Sauter mean diameter, which directly translates into a decrease in the effectiveness of PM2.5 dust reduction. The most favourable result of the PM2.5 dust reduction efficiency was obtained for the case when the water pressure was 0.1 MPa and compressed air 0.5 MPa, which corresponds to the lowest value of the Sauter mean diameter obtained by the tested combinations of the spraying parameters. The reverse situation is for the determined mean Sauter diameter and the results of the PM10 dust reduction efficiency. The obtained results show that the larger the Sauter mean diameter (D32), the greater effectiveness of PM10 dust reduction. At the same time, a decrease in the compressed air pressure in relation to water pressure increases the size of the Sauter diameter (D32), and thus increases the effectiveness of PM10 dust reduction
The results from testing the smart SSD-1 spraying device clearly indicate that the assumed objective to develop a dust reduction device that would reduce PM2.5 and PM10 dust more effectively than the currently used solutions, was achieved. The most important advantage of the new solution of the SSD-1 device is that the effectiveness of PM10 and PM2.5 dust reduction in nearly the same unlike the known spraying devices. As a result, the device, unlike previous solutions, does not reduce effectively only one type of dust, so the device is more universal. An additional advantage of the solution is its adaptability, allowing the spraying intensity to be adjusted to the current concentration of PM10 and PM2.5 dust. This allows for obtaining the optimum spraying parameters for effective dust control and reduction of water consumption.

In the case of PM10 dust reduction, the highest efficiency (73%) was achieved with water and compressed air pressure of 0.3 MPa, and drops size D(32) of 83.41 µm. In turn, the highest efficiency of PM2.5 dust reduction (80%) was obtained at a water pressure of 0.1 MPa and a compressed air pressure of 0.3 MPa, and the drops size D(32) 43.82 µm.

Declaration of interests

The authors declare that they have no known competing financial interests or personal relationships that could have appeared to influence the work reported in this paper.

Acknowledgements
This work forms part of the 'Reducing risks from Occupational exposure to Coal Dust" (ROCD) project which is supported by the European Commission Research Fund for Coal and Steel; Grant Agreement Number - 754205.

References

[1] Bałaga, D. (2019, December). Smart spraying installation for dust control in mine workings. In IOP Conference Series: Materials Science and Engineering (Vol. 679, No. 1, p. 012019). IOP Publishing. https://doi.org/10.1088/1757-899X/679/1/012019
[2] Bałaga, D., Jaszczuk M., (2016) Wpływ parametrów strumienia zraszającego na redukcję zapylenia generowanego przez kombajn ścianowy. Prace Naukowe - Monografie KOMAG. Instytut Techniki Górniczej KOMAG nr 47.
[3] Bałaga, D., Jedziniak, M., Kalita, M., Siegmund, M., & Szkudlarek, Z. (2015). Metody i środki zwalczania zagrożeń pyłowych i metanowych w górnictwie węglowym. Maszyny Górnicze, 33.
[4] Bałaga, D., Kalita, M., & Siegmund, M. (2019, May). Analysis of fraction distribution of the water drops stream generated by the spraying nozzles of new KOMAG design. In IOP Conference Series: Materials Science and Engineering (Vol. 545, No. 1, p. 012010). IOP Publishing. https://doi.org/10.1088/1757-899X/545/1/012010.
[5] Brodny, J., & Tutak, M. (2018). Exposure to harmful dusts on fully powered longwall coal mines in Poland. International Journal of Environmental Research and Public Health, 15(9), 1846.
[6] Changchi Y., Zhizong C., Dewen, L. (1996). Prace naukowe i badania nad zwalczaniem zapylenia za pomocą wentylacji w zmechanizowanych przodkach chodnikowych chińskich kopalń węgla. Międzynarodowa Konferencja Naukowo Techniczna U. S. Departament of Energy i KOMAG: „Zwalczanie zagrożeń pyłowych w przemyśle górniczym na świecie". Szczyrk
[7] Cohen R.A., Petsonk E.L., Rose C., Young B., Regier M., Najmuddin A., Abraham J.L., Churg A., Green F.H. (2018) Lung Pathology in U.S. Coal Workers with Rapidly Progressive Pneumoconiosis Implicates Silica and Silicates. Am J Respir Crit Care Med. Mar 15; 193(6): pp. 673-80. https://doi.org/10.1164/rccm.201505-1014OC
[8] Cybulski K. (2005).Zagrożenie wybuchem pyłu węglowego oraz ocena skuteczności działań profilaktycznych w polskich kopalniach węgla kamiennego. Prace Naukowe Głównego Instytutu Górnictwa No. 864. Główny Instytut Górnictwa. Katowice.
[9] Cybulski, W. (1973). Wybuchy pyłu węglowego i ich zwalczanie. Wydawnictwo" Śląsk".

[10] Ding, J., Zhou, G., Liu, D., Jiang, W., Wei, Z., & Dong, X. (2020). Synthesis and performance of a novel high-efficiency coal dust suppressant based on self-healing gel. Environmental Science & Technology, 54(13), 7992-8000. https://doi.org/10.1021/acs.est.0c00613.

[11] Górniczy, W. U. (2020). Ocena stanu bezpieczeństwa pracy, ratownictwa górniczego oraz bezpieczeństwa powszechnego w związku z działalnością górniczo-geologiczną w 2019 roku. Wyższy Urząd Górniczy. Katowice.

[12] Karowiec, K. (1984). Zwalczanie zapylenia za pomocą wyrzutu strumienia powietrza nasyconego mgłą wodną na źródło pyłu. Maszyny Górnicze. Urządzenia Odpylające, (5).

[13] Landen, D. D., Wassell, J. T., McWilliams, L., & Patel, A. (2011). Coal dust exposure and mortality from ischemic heart disease among a cohort of US coal miners. American journal of industrial medicine, 54(10), 727-733.

[14] Laskowski, T. (1948). Zagadnienie przeróbki miału w polskim przemyśle węglowym. Biuro Wydawnictw Technicznych CZPW.

[15] Lebecki, K., Cybulski, K., & Szulik, A. (2004, February). Risk of Coal Dust Explosion and its Elimination. In International Mining Forum 2004, New Technologies in Underground Mining, Safety in Mines: Proceedings of the Fifth International Mining Forum 2004, Cracow-Szczyrk-Wieliczka, Poland (p. 203).

[16] Li, S., Zhou, G., Liu, Z., Wang, N., Wei, Z., & Liu, W. (2020). Synthesis and performance characteristics of a new ecofriendly crust-dust suppressant extracted from waste paper for surface mines. Journal of Cleaner Production, 258, 120620. https://doi.org/10.1016/j.jclepro.2020.120620

[17] Libera, K., Puchała, B., Prostański, D., & Bałaga, D. (2010). Innowacyjne rozwiązania systemu zraszania powietrzno-wodnego w kombajnach chodnikowych produkcji REMAG-u. Problemy Bezpieczeństwa w Budowie i Eksploatacji Maszyn i Urządzeń Górnictwa Podziemnego, 105-114.

[18] Liu, R. Chen, F. Sera, A.M. Vicedo-Cabrera, Y. Guo, S. Tong, M.S.Z.S. Coelho, P.H.N. Saldiva, E. Lavigne, P. Matus, O.N. Valdes, G.S. Osorio, M. Pascal, M. Stafoggia, M. Scortichini, M. Hashizume, Y. Honda, M. Hurtado-Díaz, J. Cruz, B. Nunes, J.P. Teixeira, H. Kim, A. Tobias, C. Íñiguez, B. Forsberg, C. Åström, M.S. Ragettli, Y.L. Guo, B.Y. Chen, M.L. Bell, C.Y. Wright, N. Scovronick, R.M. Garland, A. Milojevic, J. Kyselý, A. Urban, H. Orru, E. Indermitte, J.J.K. Jaakkola, N.R.I. Ryti, K. Katsouyanni, A. Analitis, A. Zanobetti, J. Schwartz, J. Chen, T. Wu, A. Cohen, A. Gasparrini, H. Kan, 2019. Ambient Particulate Air Pollution and Daily Mortality in 652 Cities. N. Engl. J. Med., 381, 705-715. https://doi.org/10.1056/NEJMoa1817364

[19] Liu, R., Zhou, G., Wang, C., Jiang, W., & Wei, X. (2020). Preparation and performance characteristics of an environmentally-friendly agglomerant to improve the dry dust removal effect for filter material. Journal of Hazardous Materials, 122734. https://doi.org/10.1016/j.jhazmat.2020.122734

[20] Liu, Z., Nie, W., Peng, H., Yang, S., Chen, D., & Liu, Q. (2019). The effects of the spraying pressure and nozzle orifice diameter on the atomizing rules and dust suppression performances of an external spraying system in a fully-mechanized excavation face. Powder Technology, 350, 62-80. https://doi.org/10.1016/j.powtec.2019.03.029

[21] Ma, Q., Nie, W., Yang, S., Xu, C., Peng, H., Liu, Z., ... & Cai, X. (2020). Effect of spraying on coal dust diffusion in a coal mine based on a numerical simulation. *Environmental Pollution*, 114717. https://doi.org/10.1016/j.envpol.2020.114717

[22] NIOSH, 2019. Mining Topic: Respiratory Diseases - What is the health and safety problem? Available at: https://www.cdc.gov/niosh/mining/topics/RespiratoryDiseases.html [Accessed 17 February. 2020].

[23] PN-91/Z-04030/05:1991 Ochrona czystości powietrza. Badania zawartości pyłu. Oznaczanie pyłu całkowitego na stanowiskach pracy metodą filtracyjno-wagową. Warszawa 1991 r

[24] PN-91/Z-04030/06:1991 Ochrona czystości powietrza. Badania zawartości pyłu. Oznaczanie pyłu respirabilnego na stanowiskach pracy metodą filtracyjno-wagową. Warszawa 1991 r.

[25] Prostański, D. (2018). Development of research work in the air-water spraying area for reduction of methane and coal dust explosion hazard as well as for dust control in the Polish mining industry. Mater. Sci. Eng, 427, 012026. https://doi.org/10.1088/1757-899X/427/1/012026

[26] Ren, W., Wang, D., Guo, Q., & Zuo, B. (2014). Application of foam technology for dust control in underground coal mine. International Journal of Mining Science and Technology, 24(1), 13-16. https://doi.org/10.1016/j.ijmst.2013.12.003

[27] Rojek, P., & Kalukiewicz, A. (2012). Zastosowanie aerozolu powietrzno-wodnego dla redukcji zapylenia powietrza kopalnianego. Instytut Techniki Górniczej KOMAG.

[28] Shi, X. X., & Jiang, Z. A. (2005). Research status and development tendency of dust-control technique in the fully-mechanized mining faces in coal mine. J. Saf. Sci. Technol, 2, 41-43.
[29] Siegmund, M., Bałaga, D., & Kalita, M. (2018). Badania parametrów strumieni zraszających dysz drobnokroplistych. Maszyny Górnicze, 36.
[30] System kurtyn mgłowych może ograniczać zapylenie w kopalniach. [online] wnp.pl górnictwo. Available at: https://www.wnp.pl/gornictwo/system-kurtyn-mglowych-moze-ograniczac-zapylenie-w-kopalniach,104882.html [Accessed 20 January. 2020].
[31] Świątkowska, B., & Hanke, W. (2018). OCCUPATIONAL DISEASES IN POLAND IN 2016/CHOROBY ZAWODOWE W POLSCE W 2016 ROKU. Medycyna pracy, 69(6), 643-651.
[32] Wang, H., Du, Y., Wei, X., & He, X. (2019). An experimental comparison of the spray performance of typical water-based dust reduction media. Powder Technology, 345, 580-588. https://doi.org/10.1016/j.powtec.2019.01.032
[33] Wang, P., Tan, X., Zhang, L., Li, Y., & Liu, R. (2019). Influence of particle diameter on the wettability of coal dust and the dust suppression efficiency via spraying. Process Safety and Environmental Protection, 132, 189-199. https://doi.org/10.1016/j.psep.2019.09.031
[34] Xu, C., Nie, W., Liu, Z., Peng, H., Yang, S., & Liu, Q. (2019). Multi-factor numerical simulation study on spray dust suppression device in coal mining process. *Energy*, *182*, 544-558.https://doi.org/10.1016/j.energy.2019.05.201
[35] Zacharzewski J., Kwiecień Z. (1974). Kryterium efektywności strącania pyłów z powietrza kopalnianego kroplami rozpylonej wody. Sympozjum Naukowe Zwalczanie zapylenia powietrza kopalnianego, Katowice